C. R. Mecanique 346 (2018) 366–383

Contents lists available at ScienceDirect

Comptes Rendus Mecanique

www.sciencedirect.com

Unsteady free surface flow in porous media: One-dimensional model equations including vertical effects and seepage face

Carmine Di Nucci

Civil, Construction-Architectural and Environmental Engineering Department – University of L'Aquila, Via Giovanni Gronchi 18, Zona industriale di Pile, 67100 L'Aquila, Italy

ARTICLE INFO

Article history:
Received 17 March 2017
Accepted 6 March 2018
Available online 16 March 2018

Keywords:
Boussinesq-type model
Nonlinear water waves
Porous medium
Seepage face
Rectangular dam

ABSTRACT

This note examines the two-dimensional unsteady isothermal free surface flow of an incompressible fluid in a non-deformable, homogeneous, isotropic, and saturated porous medium (with zero recharge and neglecting capillary effects). Coupling a Boussinesq-type model for nonlinear water waves with Darcy's law, the two-dimensional flow problem is solved using one-dimensional model equations including vertical effects and seepage face. In order to take into account the seepage face development, the system equations (given by the continuity and momentum equations) are completed by an integral relation (deduced from the Cauchy theorem). After testing the model against data sets available in the literature, some numerical simulations, concerning the unsteady flow through a rectangular dam (with an impermeable horizontal bottom), are presented and discussed.

1. Introduction

The Boussinesq equation [1–4] is the prototype of one-dimensional model equations for the study of unsteady free surface flow in porous media. As is well known, this equation can be obtained by coupling the Dupuit approximation with the Darcy law. To investigate how the flow is affected by vertical velocity, the Boussinesq equation is often replaced by a series of extended Boussinesq equations [5–12]. These equations are used extensively to describe the water waves propagation in porous media as a consequence of tide-induced fluctuations [5–10] and wave interactions with porous structures [7,11,12]. A problem arising from the use of these extended Boussinesq equations is that the seepage face development and the capillary fringe effects are neglected. Whereas a series of alternative Boussinesq equations are proposed to evaluate the capillary fringe effects [13–15], how to evaluate the seepage face development with a one-dimensional model is a problem still not completely solved [16,17].

An attempt to determine the height of the seepage face with the Boussinesq equation is performed in [16] by incorporating in the model equation a new equation. However, this equation, expressed by an inequality, "*is an intuitive approximation of how a seepage face could form assuming Dupuit–Forchheimer flow*" [16]. In the light of this statement, the use of this inequality in conjunction with the Boussinesq equation must be considered as a mathematical artifice that is used to force fit the model predictions to experimental evidences. This kind of approaches, based on mathematical models of dubious physical meaning, is commonly used also in other field (e.g., open channel flow and pipe flow – a critical review can be found in [18–25]), and determines a dangerous separation between the obtained solution and the problem under investigation.

E-mail address: carmine.dinucci@univaq.it.

https://doi.org/10.1016/j.crme.2018.03.003
1631-0721/

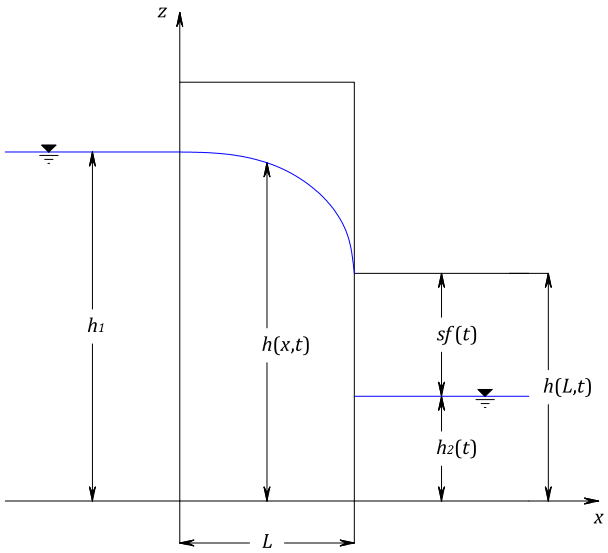

Fig. 1. Definition sketch.

In steady-state flow conditions, the seepage face height is evaluated analytically in a simple configuration (seepage flow in a homogeneous rectangular dam) by Polubarinova-Kochina [26]. This analytical solution, given in the elliptic integral form of the first kind, is computed numerically in [27]. For some simple configurations, approximate methods to compute the seepage face height can be found in [28–33].

In the field of numerical models, the seepage face problem is analyzed, among others, in [34–42].

Within the framework of extended Boussinesq equations (in the above-mentioned meaning), this note proposes a new set of one-dimensional model equations including vertical effects and seepage face. The model is built considering the archetypal case of the two-dimensional unsteady isothermal flow of an incompressible fluid in a non-deformable, homogeneous, isotropic, and saturated rectangular dam (with an impermeable horizontal bottom and zero recharge). The capillary effects are neglected. In order to take into account the seepage face development, the model equations (obtained by coupling a Boussinesq-type model for nonlinear water waves with Darcy's law) are completed by an integral relation (deduced from the Cauchy theorem). After testing the model against data sets available in the literature, some numerical simulations are presented and discussed.

The note is structured as follows: Section 1 presents the problem formulation; Section 2 is devoted to the one-dimensional model equations; the details of numerical simulations and discussions of the results are provided in Section 3; conclusions are given in Section 4. In order to make reading easier, some mathematical considerations are included in the Appendixes at the end of the paper.

2. Flow problem and governing equations

The free boundary problem under consideration concerns the two-dimensional unsteady isothermal free surface flow of an incompressible fluid (water) in a non-deformable, homogeneous, isotropic and saturated rectangular dam of width L, with an impermeable horizontal bottom. Fig. 1 shows the geometric setup: the horizontal x-axis and the vertical z-axis form a Cartesian coordinate system; t is the time variable; $h_1 =$ constant and $h_2(t)$ are, respectively, the water levels at $x = 0$ and $x = L$; $h(x,t)$ is the free surface elevation; $sf(t) = h(L,t) - h_2(t)$ is the seepage face height.

With zero recharge and neglecting the capillary effects, the free surface is a sharp interface between saturated and dry zones. The flow problem consists in finding the evolution of the free surface $h(x,t)$, the seepage velocity field $\boldsymbol{v}(x,z,t) = (v_x, v_z)$ (where $v_x(x,z,t)$ and $v_z(x,z,t)$ are the horizontal and vertical seepage velocity components, respectively) and the pressure field $p(x,z,t)$ in the unbounded flow domain $\Omega = [0,L] \times [0,h]$ for any $t > 0$.

The problem is governed by the continuity and momentum equations with appropriate boundary and initial conditions. In the range of validity of Darcy's hypothesis [43], the system equations are given as [2,43]:

$$\nabla \cdot \boldsymbol{v} = 0 \quad \text{in } \Omega \text{ (continuity equation)} \tag{1}$$

$$\boldsymbol{v} = -K\nabla\left(z + \frac{p}{\rho g}\right) \quad \text{in } \Omega \text{ (momentum equation)} \tag{2}$$

where K is the constant hydraulic conductivity, ρ the constant water density, and g the gravitational acceleration. It is important to note that the assumption of non-deformable porous medium implies that the storativity vanishes.

Eqs. (1) and (2) are subject to the following boundary conditions [2,44,45]:

$$p = 0 \quad \text{on } z = h \tag{3}$$

$$v_z = v_x \frac{\partial h}{\partial x} + \eta \frac{\partial h}{\partial t} \quad \text{on } z = h \tag{4}$$

$$v_z = 0 \quad \text{on } z = 0 \tag{5}$$

$$p = 0 \quad \text{on } x = L \text{ and } h_2 < z \leq h \tag{6}$$

$$z + \frac{p}{\rho g} = h_1 \quad \text{on } x = 0 \tag{7}$$

$$z + \frac{p}{\rho g} = h_2(t) \quad \text{on } x = L \text{ and } 0 \leq z \leq h_2 \tag{8}$$

where η is the constant porosity. Eqs. (3) and (4) are the dynamic and kinematic boundary conditions on the free surface, respectively; Eq. (5) is the kinematic boundary condition on the bottom; Eq. (6) is the seepage face boundary condition; Eqs. (7) and (8) impose the hydrostatic boundary conditions.

As is well known (see, e.g., [2,46–48]), as $h(x,t)$ is unknown, the free surface boundary conditions (3) and (4) are not redundant. Roughly speaking, the kinematic boundary condition (4) guarantees that the same particles remain on the free surface at all time [2].

In the standard approach, the flow problem is formulated in terms of the potential function $\varphi = z + p/\rho g$. By combining the continuity and momentum equations, the governing equation is expressed by the Laplace equation:

$$\nabla^2 \varphi = 0 \quad \text{in } \Omega \tag{9}$$

The boundary conditions become [2,44,45]:

$$\varphi = z \quad \text{on } z = h \tag{10}$$

$$\frac{\partial \varphi}{\partial z} = \frac{\partial \varphi}{\partial x}\frac{\partial h}{\partial x} - \frac{\eta}{K}\frac{\partial h}{\partial t} \quad \text{on } z = h \tag{11}$$

$$\frac{\partial \varphi}{\partial z} = 0 \quad \text{on } z = 0 \tag{12}$$

$$\varphi = z \quad \text{on } x = L \text{ and } h_2 < z \leq h \tag{13}$$

$$\varphi = h_1 \quad \text{on } x = 0 \tag{14}$$

$$\varphi = h_2(t) \quad \text{on } x = L \text{ and } 0 \leq z \leq h_2 \tag{15}$$

By introducing the stream function ψ given as:

$$v_x = \frac{\partial \psi}{\partial z} \tag{16}$$

$$v_z = -\frac{\partial \psi}{\partial x} \tag{17}$$

the following relationships hold:

$$\nabla^2 \psi = 0 \quad \text{in } \Omega \tag{18}$$

$$\psi = q \quad \text{on } z = h \tag{19}$$

$$\psi = 0 \quad \text{on } z = 0 \tag{20}$$

$$-\frac{\partial \psi}{\partial x} = \frac{\partial \psi}{\partial z}\frac{\partial h}{\partial x} + \eta \frac{\partial h}{\partial t} \quad \text{on } z = h \tag{21}$$

where $q(x,t)$ is the unit discharge.

The recall of these three formulations of the problem (in terms of $\boldsymbol{v}$ and p – Eqs. (1)–(8) –, in terms of the potential function φ – Eqs. (9)–(15) –, and in terms of the stream function ψ – Eqs. (18)–(21)) are presented for the sake of completeness. Moreover, some of these equations are also used to develop the one-dimensional model.

For further developments, it is also useful to note that at any time t, the two functions φ and ψ satisfy the Cauchy–Riemann relations:

$$\frac{\partial \varphi}{\partial x} = -\frac{1}{K}\frac{\partial \psi}{\partial z} \tag{22}$$

$$\frac{\partial \varphi}{\partial z} = \frac{1}{K}\frac{\partial \psi}{\partial x} \tag{23}$$

and the Cauchy integral relation:

$$\oint_{C^+}\left(\varphi \mathrm{d}z - \frac{1}{K}\psi \mathrm{d}x\right) = 0 \tag{24}$$

where C^+ is an oriented simple closed curve in Ω. As shown in Appendix A, Eq. (24) can be easily deduced from the Cauchy theorem [49,50].

3. One-dimensional model equations

The one-dimensional model equations are derived using a Boussinesq-type model for nonlinear water waves. The starting point is the Rayleigh expansion for the harmonic stream function [51–55]:

$$\psi(x,z,t) = f_1(x,t)z - \frac{1}{3!}\frac{\partial^2 f_1}{\partial x^2}z^3 + \frac{1}{5!}\frac{\partial^4 f_1}{\partial x^4}z^5 - \frac{1}{7!}\frac{\partial^6 f_1}{\partial x^6}z^7 + \dots \tag{25}$$

where $f_1(x,t)$ is an arbitrary function.

As is well known, this expansion is only formal, and it is not necessary to justify the convergence of the sum with two or three terms [56]. Following the procedure proposed by Benjamin et al. (1954) [51], neglecting all terms after the first two, the stream function can be expressed as (see Appendix B):

$$\psi(x,z,t) = \frac{q}{h}z - \frac{1}{3!}\frac{\partial^2}{\partial x^2}\left(\frac{q}{h}\right)\left(z^3 - h^2 z\right) \tag{26}$$

To the same order of approximation, the potential function is given as:

$$\varphi(x,z,t) = h - \frac{1}{2K}\frac{\partial}{\partial x}\left(\frac{q}{h}\right)\left(h^2 - z^2\right) \tag{27}$$

Eq. (27) is obtained by vertical integration of Eq. (23):

$$\frac{\partial \varphi}{\partial z} = \frac{1}{K}\frac{\partial \psi}{\partial x} = \frac{1}{K}\frac{\partial}{\partial x}\left(\frac{q}{h}\right)z \tag{28}$$

and using the dynamic condition (10).

In accordance with Eqs. (26) and (27), Eq. (22) provides the following one-dimensional momentum equation:

$$\frac{q}{K} = -\frac{\partial}{\partial x}\left[\frac{h^2}{2} - \frac{1}{K}\frac{\partial}{\partial x}\left(\frac{q}{h}\right)\frac{h^3}{3}\right] \tag{29}$$

while the kinematic boundary condition (4) becomes the one-dimensional continuity equation (see Appendix C):

$$\frac{1}{K}\frac{\partial q}{\partial x} = -\frac{\eta}{K}\frac{\partial h}{\partial t} \tag{30}$$

The system equations (29) and (30) can be solved with appropriate initial and boundary conditions.

Although these aspects are considered in more detail later, it is important to start a discussion about the boundary conditions.

Similarly as for the 2D problem, at $x = 0$ the boundary condition is given as:

$$h(0,t) = h_1 = \text{constant} \tag{31}$$

On the contrary, at $x = L$ the boundary condition cannot be expressed in term of $h_2(t)$: the 1D model provides $h(x,t)$ and $q(x,t)$, while no information on $h_2(t)$ is given. With the proposed 1D model, $h_2(t)$ and, consequently, $sf(t)$, are further unknown functions to be determined.

In the first instance, to overcome this shortcoming, at $x = L$ the boundary condition is given as:

$$\frac{q}{K}(L,t) = g(t) \tag{32}$$

where the function $g(t)$ must be set to reproduce the boundary condition of the 2D problem in the best possible way.

Once the free surface elevation $h(x,t)$ and the unit discharge $q(x,t)$ are available, the seepage velocity $\boldsymbol{v}(x,z,t) = (v_x, v_z)$ and the pressure field $p(x,z,t)$ can be evaluated as:

$$v_x(x,z,t) = -K\frac{\partial h}{\partial x}\left[1 - \frac{h}{K}\frac{\partial}{\partial x}\left(\frac{q}{h}\right)\right] + \frac{1}{2}\frac{\partial^2}{\partial x^2}\left(\frac{q}{h}\right)\left(h^2 - z^2\right) \tag{33}$$

$$v_z(x,z,t) = -\frac{\partial}{\partial x}\left(\frac{q}{h}\right)z \tag{34}$$

$$\frac{1}{\rho g}p(x,z,t) = h - z - \frac{1}{2K}\frac{\partial}{\partial x}\left(\frac{q}{h}\right)\left(h^2 - z^2\right) \tag{35}$$

The problem to compute $h_2(t)$ and $sf(t)$ can be solved using the Cauchy integral relation (24).

Identifying C^+ with the boundary of the domain Ω (taken positive in counterclockwise direction) and using the boundary conditions (10), (13), (14), (15), (19), (20), Eq. (24) becomes:

$$\oint_{C^+}\left(\varphi \mathrm{d}z - \frac{1}{K}\psi \mathrm{d}x\right) = \int_{h_1}^{0} h_1 \mathrm{d}z + \int_{0}^{h_2(t)} h_2(t)\mathrm{d}z + \int_{h_2}^{h(L,t)} z\mathrm{d}z + \int_{h(L,t)}^{h_1} z\mathrm{d}z - \int_{L}^{0}\frac{1}{K}q(x,t)\mathrm{d}x = 0 \tag{36}$$

After some rearranging, Eq. (36) takes the form:

$$\frac{1}{2}h_2^2(t) = \frac{1}{2}h_1^2 - \int_0^L \frac{1}{K}q(x,t)\mathrm{d}x \tag{37}$$

and the seepage face height can be evaluated as:

$$sf(t) = h(L,t) - h_2(t) = h(L,t) - \sqrt{h_1^2 - 2\int_0^L \frac{1}{K}q(x,t)\mathrm{d}x} \tag{38}$$

As shown in Appendix D, after some manipulations, the system equations (29) and (30) can be reduced to a one-dimensional equation in $h(x,t)$ which agree with the equations derived by Dagan (1967) [5], Parlange et al. (1984) [6], Liu et al. (1997) [7], Nielsen et al. (1997) [8]. These relationships offer insight on the order of approximation of Eqs. (29) and (30).

4. Numerical simulations

The numerical integration of system equations:

$$\frac{q}{K} = -\frac{\partial}{\partial x}\left[\frac{h^2}{2} - \frac{1}{K}\frac{\partial}{\partial x}\left(\frac{q}{h}\right)\frac{h^3}{3}\right] \tag{39}$$

$$\frac{1}{K}\frac{\partial q}{\partial x} = -\frac{\eta}{K}\frac{\partial h}{\partial t} \tag{40}$$

subject to the boundary conditions:

$$h(0,t) = h_1 = \text{constant} \tag{41}$$

$$\frac{q}{K}(L,t) = g(t) \tag{42}$$

is performed using the commercial finite element software COMSOL Multiphysics [57].

In the numerical setup, a number of 15 elements are used in the x-direction (a finer mesh did not show a considerable difference in the results). The COMSOL Multiphysics solver, based on variable-order variable-step-size backward differentiation formulas (BDF) see, e.g., [58], automatically chooses appropriate numerical time steps. The computation takes a few seconds and does not pose any special difficulties.

As mentioned above, once the free surface elevation $h(x,t)$ and the unit discharge $q(x,t)$ are computed, $h_2(t)$ and the seepage face height are evaluated by means of Eqs. (37) and (38), respectively.

The model testing is carried out by comparing the numerical results with numerical data sets, available in the literature [39], concerning the evolution of the free boundary from the static state ($h(x,0) = h_1$) until the stationary state. The value of h_1 is kept constant, while the value of h_2 passes instantaneously from $h_2(t=0) = h_1$ to a preset value $h_2(t>0) = H_2$. The geometrical and physical data sets are given in Table 1.

The proposed 1D model is able to reproduce only similar conditions (the meaning of which is explained in Appendix E) by imposing that $g(t)$ passes instantaneously from $g(t=0) = 0$ to the value $g(t>0) = q^* = \frac{h_1^2 - H_2^2}{2L}$ (see Table 1), where $q^* = \frac{h_1^2 - H_2^2}{2L}$ is the unit discharge in the stationary state (see Appendix A). In order to show the quality of the validation, the selected results are presented in Figs. 2–13.

The figures show that the stationary state is achieved more quickly using the proposed model, and that, in stationary state, the proposed model provides a free surface elevation which is always higher than that of the numerical model [39].

Table 1
Parameter setting.

Test	h_1	H_2	L	η/K	$\frac{h_1^2-H_2^2}{2L}$
1	1	0.167	0.667	0.4	0.729
2	3.22	0.84	1.62	0.2	2.982
3	4	0.84	1.62	0.2	4.720

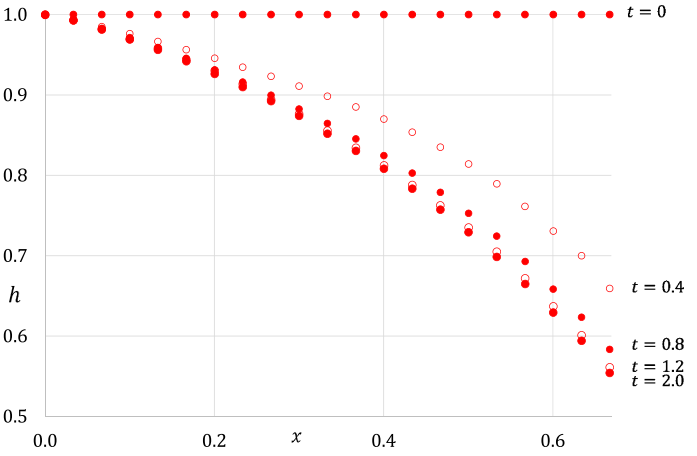

Fig. 2. Test case 1. Free surface elevations: numerical results [39].

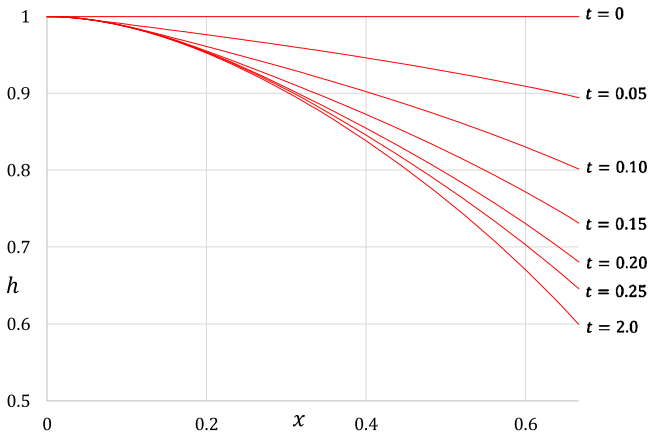

Fig. 3. Test case 1. Free surface elevations: model results.

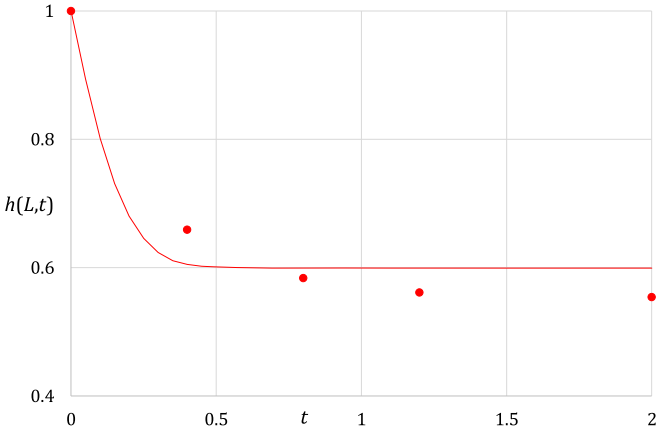

Fig. 4. Test case 1: — model results; ● numerical results [39].

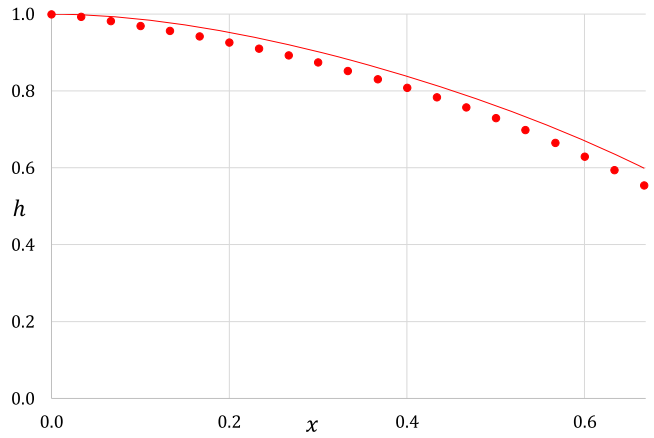

Fig. 5. Test case 1. Free surface elevations at $t = 2$; — model results; ● numerical results [39].

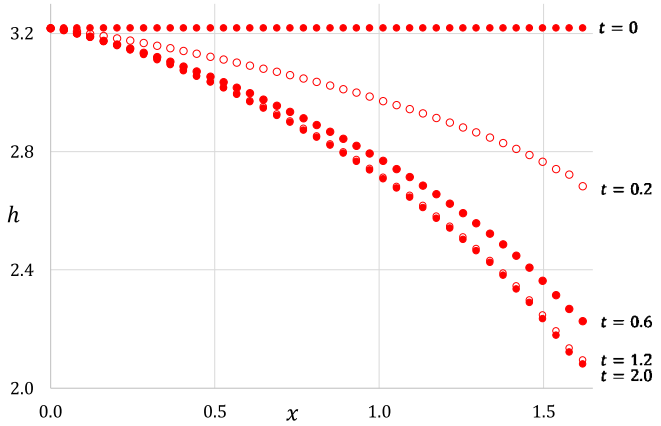

Fig. 6. Test case 2. Free surface elevations: numerical results [39].

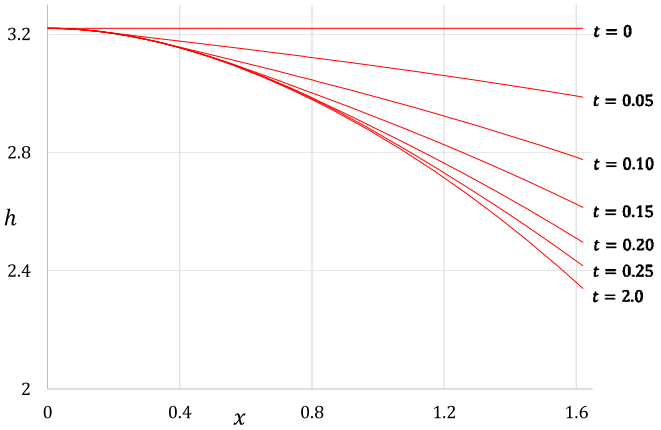

Fig. 7. Test case 2. Free surface elevations: model results.

The analysis of the results indicate that the maximum percentage error is of the order of 15 per cent.

In the following, the proposed model is applied to evaluate the influence of the several parameters on the flow process. The simulations involve 12 different scenarios that occur during a lowering of the free surface. The values of the input parameters are given in Table 2.

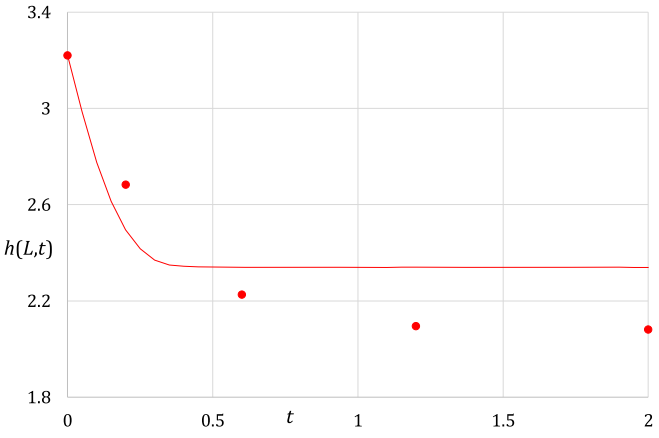

Fig. 8. Test case 2: — model results; ● numerical results [39].

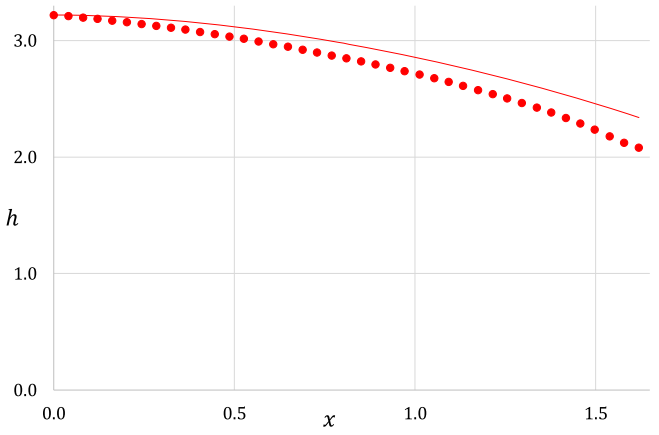

Fig. 9. Test case 2. Free surface elevations at $t = 2$; — model results; ● numerical results [39].

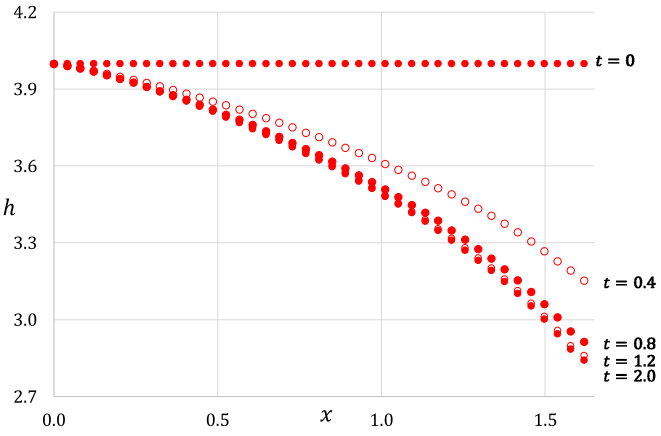

Fig. 10. Test case 3. Free surface elevations: numerical results [39].

In these simulations, the function $g(t)$, introduced by Eq. (42), is modeled using a linear step function defined by the following parameters: start time T, initial value $g(t \le T) = q_0/K$, final value $g(t \ge T + \tau) = q_f/K$, where τ is the transition time, $\frac{q_0}{K} = \frac{h_1^2 - h_{2,0}^2}{2L}$, $h_{2,0} = h_2(t = 0)$, $\frac{q_f}{K} = \frac{h_1^2 - h_{2,f}^2}{2L}$, $h_{2,f} = h_2(t \to \infty)$.

The initial conditions are given as (Appendix F):

$$\frac{q}{K}(x, 0) = \frac{q_0}{K} = \frac{h_1^2 - h_{2,0}^2}{2L} \tag{43}$$

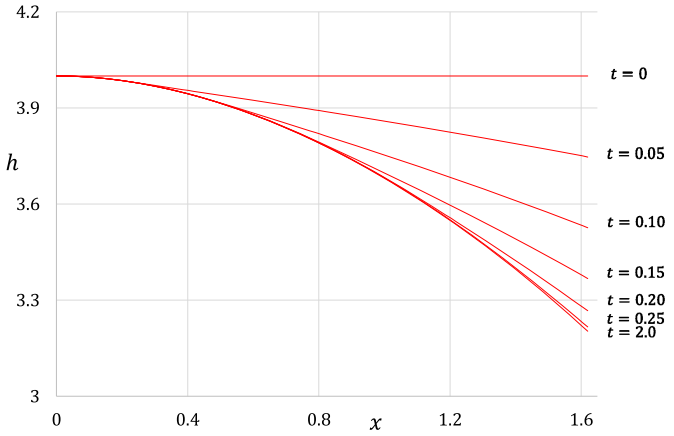

Fig. 11. Test case 3. Free surface elevations: model results.

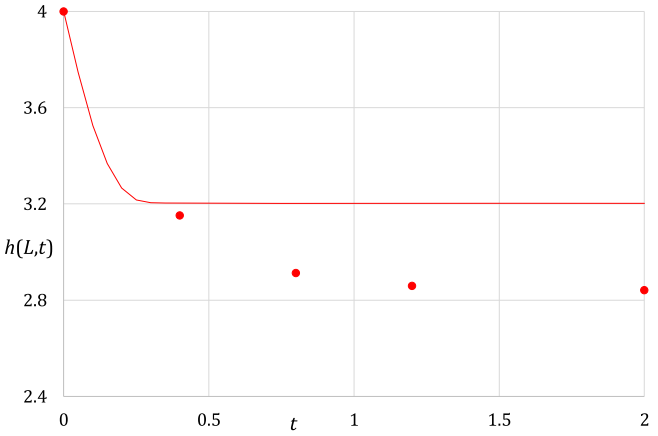

Fig. 12. Test case 3: — model results; ● numerical results [39].

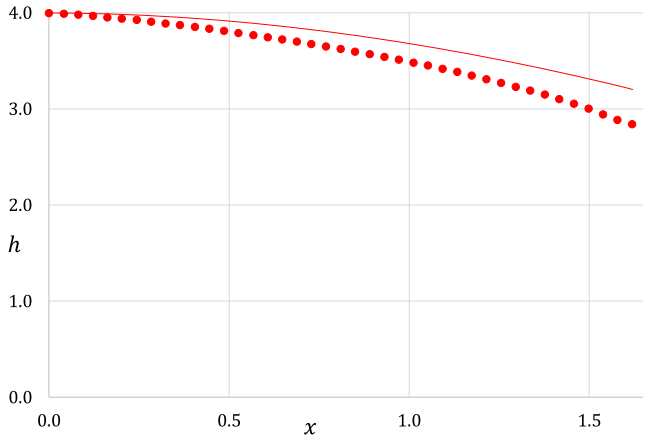

Fig. 13. Test case 3. Free surface elevations at $t = 2$; — model results; ● numerical results [39].

$$h(x,0) = \sqrt{h_1^2 - 2\frac{q_0}{K}x + \frac{2}{3}\frac{q_0^2}{K^2}\left[1 - \exp\left(-\frac{3K}{q_0}x\right)\right]} \tag{44}$$

Selected results are presented in Figs. 14–16.

Table 2
Parameter setting. For all scenarios: $h_1 = 1$, $h_{2,0} = 0.8$, $h_{2,f} = 0.1$, $T = 500$.

Scenario	η/K	τ	L
1	300	20	1
2	300	200	1
3	300	2000	1
4	3000	20	1
5	3000	200	1
6	3000	2000	1
7	300	20	0.5
8	300	200	0.5
9	300	2000	0.5
10	3000	20	0.5
11	3000	200	0.5
12	3000	2000	0.5

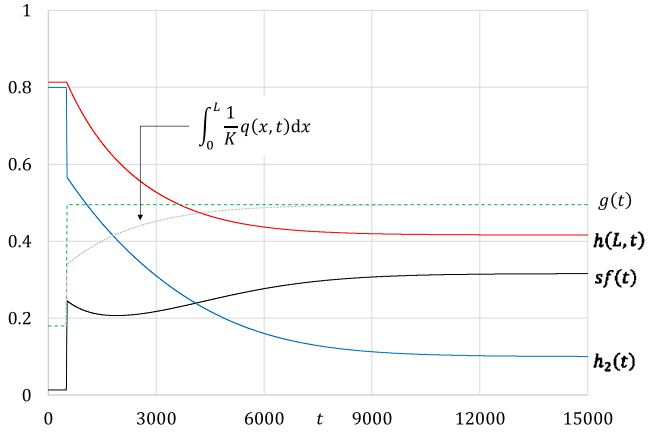

Fig. 14. Scenario 4 (see Table 2 for the parameter setting). Trends of $h(L,t)$, $sf(t)$, $\int_0^L \frac{1}{K} q(x,t)\mathrm{d}x$ and $h_2(t)$ for a given $g(t)$.

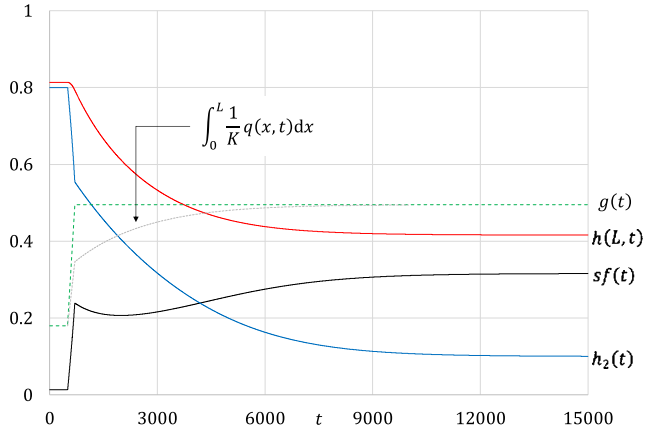

Fig. 15. Scenario 5 (see Table 2 for the parameter setting). Trends of $h(L,t)$, $sf(t)$, $\int_0^L \frac{1}{K} q(x,t)\mathrm{d}x$ and $h_2(t)$ for a given $g(t)$.

Figs. 14–16 show, among other things, that the relationships between $g(t)$ and $\int_0^L \frac{1}{K} q(x,t)\mathrm{d}x$, and between $g(t)$ and $h_2(t)$, are nonlinear; consequently, the problem under investigation cannot be adequately described by a succession of steady states.

A summary of the results is plotted in the following figures.

Figs. 17–18 show the influence of $g(t)$ and of $\frac{\eta}{K}$ on $h_2(t)$.

For the same boundary conditions, i.e. the same function $g(t)$, the influence of $\frac{\eta}{K}$ on $h_2(t)$ decreases as L decreases; the influence of $\frac{\eta}{K}$ in the evolution of the phenomenon under investigation decreases as the transition time τ of $g(t)$ increases.

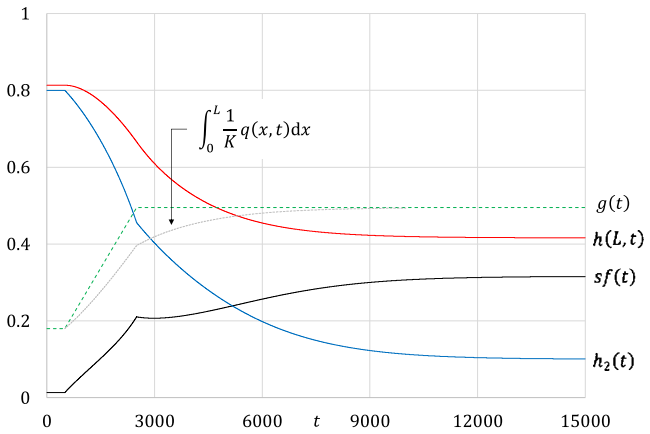

Fig. 16. Scenario 6 (see Table 2 for the parameter setting). Trends of $h(L,t)$, $sf(t)$, $\int_0^L \frac{1}{K} q(x,t)\mathrm{d}x$ and $h_2(t)$ for a given $g(t)$.

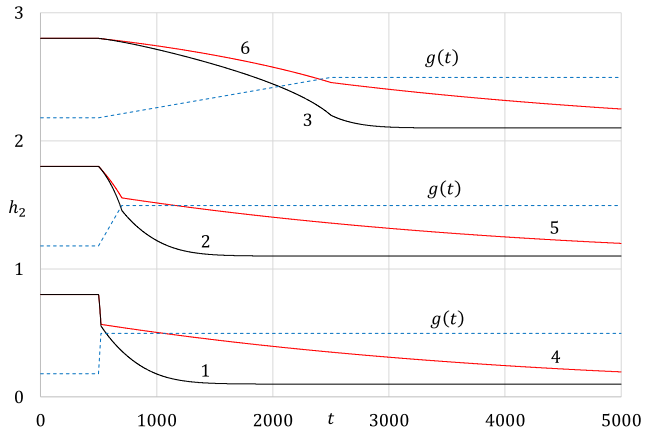

Fig. 17. Comparisons between scenario 1 and scenario 4, 2 and 5, 3 and 6 (see Table 2 for the parameter setting). The plots are shifted vertically by 1 unit.

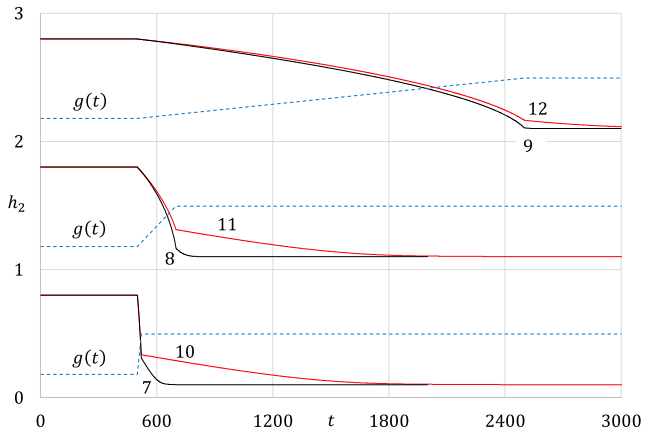

Fig. 18. Comparisons between scenario 7 and scenario 10, 8 and 11, 9 and 12 (see Table 2 for the parameter setting). The plots are shifted vertically by 1 unit.

Considering that, if $\frac{\eta}{K}$ decreases, the stationary state is achieved more quickly, and considering the usual variation range of porosity η and of hydraulic conductivity K see, e.g., [2], K played a predominant role over η in the evolution of the phenomenon under investigation.

Figs. 19–20 show the influence of $g(t)$ and of $\frac{\eta}{K}$ on $sf(t)$.

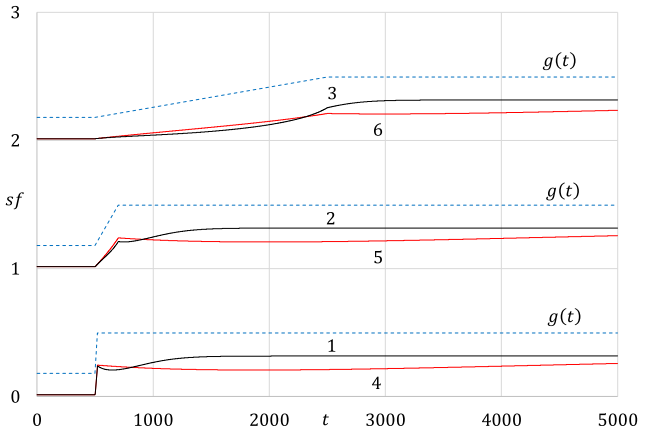

Fig. 19. Comparisons between scenario 1 and scenarios 4, 2 and 5, 3 and 6 (see Table 2 for the parameter setting). The plots are shifted vertically by 1 unit.

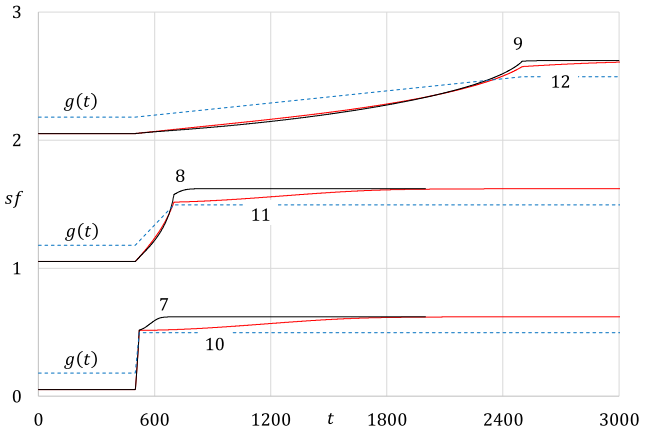

Fig. 20. Comparisons between scenario 7 and scenario 10, 8 and 11, 9 and 12 (see Table 2 for the parameter setting). The plots are shifted vertically by 1 unit.

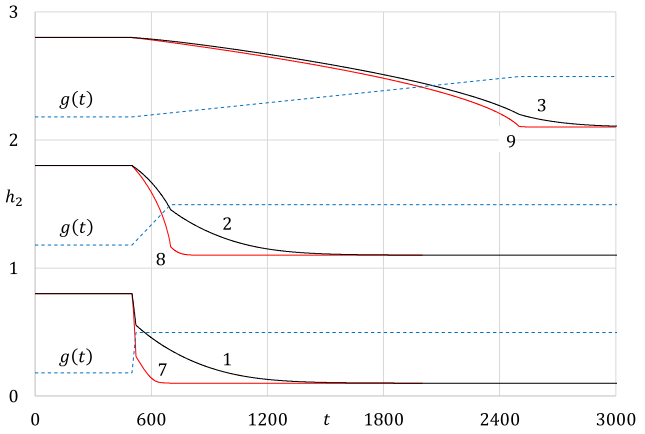

Fig. 21. Comparison between Scenario 1 and 7, 2 and 8, 3 and 9 (see Table 2 for the parameter setting). The plots are shifted vertically by 1 unit.

From a qualitative point of view, the behavior of $sf(t)$ is similar to those of $h_2(t)$: for the same boundary conditions, i.e. the same function $g(t)$, the influence of $\frac{\eta}{K}$ on $sf(t)$ decreases as L decreases. However, the influence of $\frac{\eta}{K}$ on $sf(t)$ is less than that of $\frac{\eta}{K}$ on $h_2(t)$.

Figs. 21–22 show the influence of $g(t)$ and of L on $h_2(t)$.

For the same boundary conditions, i.e. the same function $g(t)$, the influence of L on $h_2(t)$ increases as $\frac{\eta}{K}$ increases.

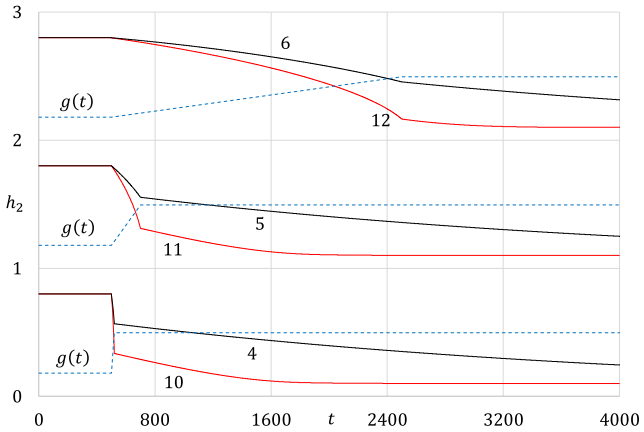

Fig. 22. Comparison between Scenario 4 and 10, 5 and 11, 6 and 12 (see Table 2 for the parameter setting). The plots are shifted vertically by 1 unit.

5. Conclusions

In this note, the two-dimensional unsteady isothermal free surface flow of an incompressible fluid in a non-deformable, homogeneous, isotropic, and saturated porous medium (with zero recharge and neglecting capillary effects) has been considered. The two-dimensional flow problem has been solved using one-dimensional model equations including vertical effects and seepage face. The vertical effects have been taken into account coupling a Boussinesq-type model for nonlinear water waves with Darcy's law. The problem to compute the seepage face height has been overcome through the use of the Cauchy integral relation. The ability to determine the seepage face, distinguishes the proposed 1D model from the previous 1D models based on the Boussinesq-equation or on the Boussinesq extended equations. The governing equations have been numerically integrated using the commercial finite element software COMSOL Multiphysics. The numerical set up is quite simple and the computation does not show any difficulty.

Within the framework of the unsteady flow through a rectangular dam, the proposed model has been tested against numerical data sets available in the literature. In terms of the free surface elevation, the maximum percentage error is of the order of 15 per cent.

In the same configuration (flow through a rectangular dam), some numerical simulations, which occur during a lowering of the free surface, have been presented and discussed. The main results can be summarized as follows: the problem under investigation cannot be adequately described by a succession of steady states; the hydraulic conductivity K played a predominant role over the porosity η; the influence of $\frac{\eta}{K}$ on $h_2(t)$ decreases as L decreases; the influence of $\frac{\eta}{K}$ decreases as the transition time τ increases; the influence of $\frac{\eta}{K}$ on $sf(t)$ decreases as L decreases; the influence of $\frac{\eta}{K}$ on $sf(t)$ is less than that of $\frac{\eta}{K}$ on $h_2(t)$; the influence of L on $h_2(t)$ increases as $\frac{\eta}{K}$ increases.

Comparison with similar 1D model equations [5–8] has been performed. Some comments about the order of approximation have been provided.

In steady flow conditions (see Appendix F), the comparison between the model results and the analytical solution of Polubarinova-Kochina [26] lead to similar conclusions to those discussed for the unsteady flow: the maximum percentage error is of the order of 15 per cent; the proposed model provides a free surface elevation which is always higher than that proposed by Polubarinova-Kochina [26].

The application of the proposed model to "real" problems requires the replacement of the boundary condition (40) (which is essentially mathematical) with by a more "physical" boundary condition: in other words, the boundary condition (40) should be expressed in terms of $h_2(t)$ and not in terms of $\frac{q}{K}(L,t)$. Despite this limit, in the current configuration the proposed model can be effectively applied to perform sensitivity analyses and to investigate the effects of several parameters on the flow process.

Appendix A

Setting a complex number as $y = x + \mathrm{i}z$, where i satisfies the rule $\mathrm{i}^2 = -1$, the Cauchy theorem can be formulated as follows [49,50]: if $f(y) = f(x + \mathrm{i}z)$ is analytic in a single connected region Ω, then the integral of $f(y)$ with respect to y along an oriented simple closed contour $C^+ \in \Omega$, must vanish:

$$\oint_{C^+} f(y)\mathrm{d}y = 0 \tag{45}$$

Putting $f(y) = \varphi(x,z) - \mathrm{i}\frac{1}{K}\psi(x,z)$, Eq. (45) provides:

$$\oint_{C^+} f(y)\mathrm{d}y = \oint_{C^+}\left(\varphi \mathrm{d}x + \frac{1}{K}\psi \mathrm{d}z\right) + \mathrm{i}\oint_{C^+}\left(\varphi \mathrm{d}z - \frac{1}{K}\psi \mathrm{d}x\right) = 0 \tag{46}$$

Eq. (24) is the imaginary part of the integral relation (46).

Note that in steady flow conditions, Eq. (37) provides the Dupuit–Forchheimer discharge formula [2,59]:

$$\frac{q}{K} = \frac{h_1^2 - h_2^2}{2L} \tag{47}$$

Appendix B

Using the Rayleigh expansion:

$$\psi(x,z,t) = f_1(x,t)z - \frac{1}{3!}\frac{\partial^2 f_1}{\partial x^2}z^3 + \frac{1}{5!}\frac{\partial^4 f_1}{\partial x^4}z^5 - \frac{1}{7!}\frac{\partial^6 f_1}{\partial x^6}z^7 + \dots \tag{48}$$

and neglecting all terms after the first two, the stream function can be expressed as:

$$\psi(x,z,t) = f_1(x,t)z - \frac{1}{3!}\frac{\partial^2 f_1}{\partial x^2}z^3 \tag{49}$$

Putting $\psi(x,h,t) = q$, Eq. (49) gives rise to the differential equation:

$$f_1(x,t) = \frac{q}{h} + \frac{1}{3!}\frac{\partial^2 f_1}{\partial x^2}h^2 \tag{50}$$

With the adopted approximations, the following relationships hold:

$$\frac{\partial}{\partial x}f_1(x,t) = \frac{\partial}{\partial x}\left(\frac{q}{h}\right) \tag{51}$$

$$\frac{\partial^2}{\partial x^2}f_1(x,t) = \frac{\partial^2}{\partial x^2}\left(\frac{q}{h}\right) \tag{52}$$

Eq. (50) can be written in approximate form as:

$$f_1(x,t) = \frac{q}{h} + \frac{1}{3!}\frac{\partial^2}{\partial x^2}\left(\frac{q}{h}\right)h^2 \tag{53}$$

and the stream function reduces to Eq. (26).

This procedure is standard and well documented (see, e.g., [51–56]).

Appendix C

With the adopted approximations, the following relationships hold:

$$v_x(x,h,t) = \frac{q}{h} - \frac{1}{3}\frac{\partial^2}{\partial x^2}\left(\frac{q}{h}\right)h^2 \tag{54}$$

$$v_z(x,h,t) = -\frac{\partial}{\partial x}\left(\frac{q}{h}\right)h \tag{55}$$

$$v_x(x,h,t)\frac{\partial h}{\partial x} = \frac{q}{h}\frac{\partial h}{\partial x} \tag{56}$$

$$v_z(x,h,t) - v_x(x,h,t)\frac{\partial h}{\partial x} = -\frac{\partial}{\partial x}\left(\frac{q}{h}\right)h - \frac{q}{h}\frac{\partial h}{\partial x} = -\frac{\partial q}{\partial x} \tag{57}$$

With Eq. (57), the kinematic boundary condition (4) reduces to Eq. (30).

Appendix D

With the adopted approximations, the term $\frac{1}{K}\frac{\partial}{\partial x}(\frac{q}{h})$ which appears in Eq. (29) can be expressed as:

$$\frac{1}{K}\frac{\partial}{\partial x}\left(\frac{q}{h}\right) = -\frac{\partial^2 h}{\partial x^2} \tag{58}$$

and consequently Eq. (29) can be written in approximate form as:

$$\frac{q}{K} = -\frac{\partial}{\partial x}\left[\frac{h^2}{2} - \frac{1}{K}\frac{\partial}{\partial x}\left(\frac{q}{h}\right)\frac{h^3}{3}\right] = -\frac{\partial}{\partial x}\left[\frac{h^2}{2} + \frac{h^3}{3}\frac{\partial^2 h}{\partial x^2}\right] \tag{59}$$

This equation, coupled with Eq. (30), provides:

$$\frac{\partial h}{\partial t} - \frac{K}{\eta}\frac{\partial^2}{\partial x^2}\left[\frac{h^2}{2} + \frac{h^3}{3}\frac{\partial^2 h}{\partial x^2}\right] = 0 \tag{60}$$

Eq. (60) agree with the one-dimensional equation derived by Nielsen et al. (1997) [8].

Putting $x = Lx'$, $t = \frac{L^2\eta}{kH}t'$, $\mu^2 = \frac{H^2}{L^2}$, $\varepsilon = \frac{a}{H}$, $h = \zeta + h_\mathrm{m}$, $h = Hh'$, $\zeta = a\zeta'$, $h_\mathrm{m} = Hh'_\mathrm{m}$, where L is the characteristic horizontal scale, H the characteristic vertical scale, a the typical amplitude of the free surface elevation, ζ the free surface elevation, h_m the mean depth, the dimensionless form of Eq. (60) is (where all primes have been omitted for convenience):

$$\frac{\partial h}{\partial t} - \frac{\partial^2}{\partial x^2}\left[\frac{h^2}{2} + \mu^2\frac{h^3}{3}\frac{\partial^2 h}{\partial x^2}\right] = 0 \tag{61}$$

or, equivalently:

$$\frac{\partial \zeta}{\partial t} - \varepsilon\frac{\partial}{\partial x}\left(\zeta\frac{\partial \zeta}{\partial x}\right) - h_\mathrm{m}\frac{\partial^2 \zeta}{\partial x^2} - \mu^2\frac{h_\mathrm{m}^3}{3}\frac{\partial^4 \zeta}{\partial x^4} = 0 \tag{62}$$

Eq. (62) agree with the one-dimensional equation derived by Liu et al. (1997) [7].

Expanding h in terms of the small parameter μ^2 as:

$$h = h_0 + \mu^2 h_1 + O(\mu^4) \tag{63}$$

Eq. (61) gives rise to the one-dimensional equations:

$$\frac{\partial h_0}{\partial t} - \frac{\partial}{\partial x}\left(h_0\frac{\partial h_0}{\partial x}\right) = O(\mu^2) \tag{64}$$

$$\frac{\partial h_1}{\partial t} - \frac{\partial^2}{\partial x^2}(h_0 h_1) - \frac{\mu^2}{3}\frac{\partial^2}{\partial x^2}\left(h_0^3\frac{\partial^2 h_0}{\partial x^2}\right) = O(\mu^4) \tag{65}$$

These equations agree with the equations derived by Dagan (1967) [5] and Parlange et al. (1984) [6].

In the light of these considerations, the system equations (29) and (30) can be written in dimensionless form as:

$$\tilde{q} = -\frac{\partial}{\partial x}\left[\frac{h^2}{2} - \mu^2\frac{\partial}{\partial x}\left(\frac{\tilde{q}}{h}\right)\frac{h^3}{3}\right] \tag{66}$$

$$\frac{\partial \tilde{q}}{\partial x} = -\frac{\partial h}{\partial t} \tag{67}$$

where $\tilde{q} = \frac{q}{K}\frac{L}{H^2}$. These relationships show that these system equations are accurate to the first order of μ^2, i.e., with a truncation error of $O(\mu^4)$.

Appendix E

The meaning of "similar conditions" is clarified by Fig. 23: when $g(t)$ passes instantaneously from $g(t=0)=0$ to the value $g(t>0) = q^* = \frac{h_1^2 - H_2^2}{2L}$, $h_2(t)$ descends rather steeply – but not instantaneously – to the level H_2. In the current configuration, $h_2(t)$ is a further unknown function to be determined and, consequently, the boundary conditions at $x = L$ cannot be expressed in terms of $h_2(t)$.

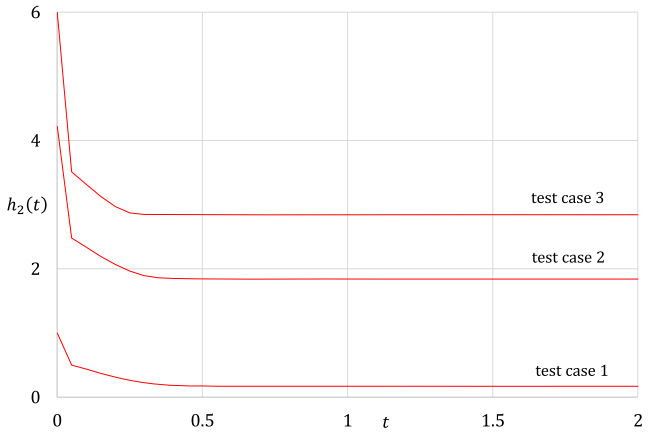

Fig. 23. Trends of $h_2(t)$ when $g(t)$ passes instantaneously from $g(t=0)=0$ to the value $g(t>0)=q^*=\frac{h_1^2-H_2^2}{2L}$. The plots are shifted vertically by 1 unit.

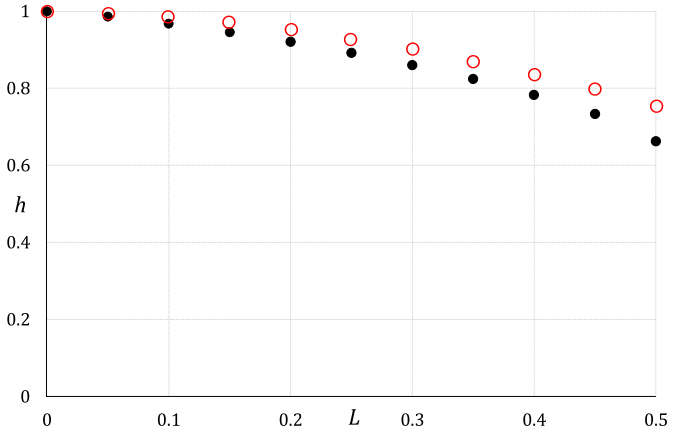

Fig. 24. Free surface elevation $h(x)$: $L=0.5$, $h_1=1$, $h_2=0.5$; ○ Eq. (72); ● numerical results [27].

Appendix F

In steady flow conditions, Eqs. (29) and (37) reduce to:

$$\frac{q}{K}=-\frac{\mathrm{d}}{\mathrm{d}x}\left(\frac{h^2}{2}+\frac{q}{K}\frac{\mathrm{d}h}{\mathrm{d}x}\frac{h}{3}\right) \tag{68}$$

$$\frac{q}{K}=\frac{h_1^2-h_2^2}{2L} \tag{69}$$

Eq. (68), subject to the following boundary conditions [2]:

$$h|_{x=0}=h_1 \tag{70}$$

$$\left.\frac{\mathrm{d}h}{\mathrm{d}x}\right|_{x=0}=0 \tag{71}$$

provides [31]:

$$h(x)=\sqrt{h_1^2-2\frac{q}{K}x+\frac{2}{3}\frac{q^2}{K^2}\left[1-\exp\left(-\frac{3K}{q}x\right)\right]} \tag{72}$$

Coupling this equation with Eq. (69), the seepage face height $sf=h(L)-h_2$ is expressed as:

$$sf=\frac{\frac{2q^2}{3K^2}(1-\mathrm{e}^{-\frac{3K}{q}L})}{h(L)+h_2} \tag{73}$$

Eq. (72) can be used to evaluate the accuracy of the proposed model in steady flow conditions. The accuracy is checked by comparison with the analytical solution proposed by Polubarinova-Kochina [26]. This solution, given in the elliptic integral form of the first kind, is computed numerically in [27].

The analysis of the results indicates that the maximum percentage error is of the order of 15 per cent, and that the Eq. (72) provides a free surface elevation which is always higher than that proposed by Polubarinova-Kochina [26]. These results are similar to those discussed above for the unsteady flow.

As examples, Fig. 24 shows the comparison between approximate (Eq. (72)) and numerical [27] free surface elevation $h(x)$.

References

[1] J. Boussinesq, Recherches théoriques sur l'écoulement des nappes d'eau infiltrées dans le sol et sur le debit des sources, J. Math. Pures Appl. 10 (1904) 5–78.
[2] J. Bear, The Dynamics of Fluids in Porous Media, Dover, New York, 1988.
[3] P.K. Mishra, K.L. Kuhlman, Unconfined Aquifer Flow Theory: From Dupuit to Present, Springer, New York, 2013.
[4] P.A. Troch, C. Paniconi, E.E. van Loon, Hillslope-storage Boussinesq model for subsurface flow and variable source areas along complex hillslopes: 1. Formulation and characteristic response, Water Resour. Res. 39 (2003) 1316.
[5] G. Dagan, Second order theory of shallow free surface flow in porous media, Q. J. Mech. Appl. Math. 20 (1967) 517–526.
[6] J.-Y. Parlange, F. Stagnitti, J.L. Starr, R.D. Braddock, Free-surface flow in porous media and periodic solution of the shallow-flow approximation, J. Hydrol. 70 (1984) 251–263.
[7] P.L.-F. Liu, J. Wen, Nonlinear diffusive surface waves in porous media, J. Fluid Mech. 347 (1997) 119–139.
[8] P. Nielsen, R. Aseervatham, J.D. Fenton, P. Perrochet, Groundwater waves in aquifers of intermediate depths, Adv. Water Resour. 20 (1997) 37–43.
[9] H.T. Teo, D.S. Jeng, B.R. Seymour, D.A. Barry, L. Li, A new analytical solution for water table fluctuations in coastal aquifers with sloping beaches, Adv. Water Resour. 26 (2003) 1239–1247.
[10] D.-S. Jeng, B.R. Seymour, D.A. Barry, J.-Y. Parlange, D.A. Lockington, L. Li, Steepness expansion for free surface flows in coastal aquifers, J. Hydrol. 309 (2005) 85–92.
[11] S. Hsiao, K. Hu, H. Hwung, Extended Boussinesq equations for water-wave propagation in porous media, J. Eng. Mech. 136 (2010) 625–640.
[12] C. Lee, V.N. Vu, T.H. Jung, Extended Boussinesq equations for waves in porous media: derivation of governing equations and generation of waves internally, in: 34th International Conference on Coastal Engineering, Seoul, Korea, 2014.
[13] J.-Y. Parlange, W. Brutsaert, A capillarity correction for free surface flow of groundwater, Water Resour. Res. 23 (1987) 805–808.
[14] L. Li, D.A. Barry, F. Stagnitti, J.-Y. Parlange, Groundwater waves in a coastal aquifer: a new governing equation including vertical effects and capillarity, Water Resour. Res. 36 (2000) 411–420.
[15] J. Kong, Z. Luo, C. Shen, G. Hua, H. Zhao, An alternative Boussinesq equation considering the effect of hysteresis on coastal groundwater waves, Hydrol. Process. 30 (2016) 2657–2670.
[16] A.J. Baird, T.E. Mason, D.P. Horn, Validation of a Boussinesq model of beach ground water behaviour, Mar. Geol. 148 (1998) 55–69.
[17] B. Raubenheimer, R.T. Guza, S. Elgar, Tidal water table fluctuations in a sandy ocean beach, Water Resour. Res. 35 (1999) 2313–2320.
[18] C. Di Nucci, A. Russo Spena, Curved-streamline transitional flow from mild to steep slopes, J. Hydraulic Res. 48 (2010) 699–700.
[19] C. Di Nucci, A. Russo Spena, Energy and momentum under critical flow condition, J. Hydraulic Res. 49 (2011) 127–128.
[20] C. Di Nucci, M. Petrilli, A. Russo Spena, Unsteady friction and visco-elasticity in pipe fluid transients, J. Hydraulic Res. 49 (2011) 398–401.
[21] C. Di Nucci, A. Russo Spena, Weakly undular hydraulic jump: effects of friction, J. Hydraulic Res. 49 (2011) 409–412.
[22] C. Di Nucci, A. Russo Spena, Moment of momentum equation for curvilinear free-surface flow, J. Hydraulic Res. 49 (2011) 415–419.
[23] C. Di Nucci, A. Russo Spena, Universal probability distributions of turbulence in open channel flows, J. Hydraulic Res. 49 (2011) 702.
[24] C. Di Nucci, A. Russo Spena, On the propagation of one-dimensional acoustic waves in liquids, Meccanica 48 (2013) 15–21.
[25] C. Di Nucci, A. Russo Spena, On transient liquid flow, Meccanica 51 (2016) 2135–2143.
[26] P. Polubarinova-Kochina, Theory of Ground Water Movement, Princeton University Press, Princeton, 1962.
[27] U. Hornung, T. Krueger, Evaluation of the Polubarinova-Kochina formula for the dam problem, Water Resour. Res. 21 (1985) 395–398.
[28] E. Bresciani, P. Davy, J.-R. de Dreuzy, Is the Dupuit assumption suitable for predicting the groundwater seepage area in hillslopes?, Water Resources Research 50 (2014) 2394–2406.
[29] C. Di Nucci, A free boundary problem: steady axisymmetric potential flow, Meccanica 48 (2013) 1805–1810.
[30] C. Di Nucci, Erratum: a free boundary problem: steady axisymmetric potential flow, Meccanica 49 (2014) 253.
[31] C. Di Nucci, Steady free-surface flow in porous media: generalized Dupuit–Fawer equations, J. Hydraul. Res. 49 (2011) 821–823.
[32] D. Chenaf, R.P. Chapuis, Seepage face height, water table position, and well efficiency at steady state, Ground Water 45 (2007) 168–177.
[33] K.R. Rushton, E.G. Youngs, Drainage of recharge to symmetrically located downstream boundaries with special reference to seepage faces, J. Hydrol. 380 (2010) 94–103.
[34] M. Todsen, On the solution of transient free-surface flow problems in porous media by finite-difference methods, J. Hydrol. 12 (1971) 177–210.
[35] R.T.-S. Cheng, C.-Y. Li, On the solution of transient free-surface flow problems in porous media by the finite element method, J. Hydrol. 20 (1973) 49–63.
[36] S.T. Potter, W.J. Gburek, Seepage face simulation using PLASM, Ground Water 25 (1987) 722–732.
[37] M.G. McDonald, A.W. Harbaugh, A Modular Three-Dimensional Finite-Difference Ground–Water Flow Model: U.S. Geological Survey Techniques of Water-Resources Investigations, 1988, book 6, Chap. A1.
[38] O. Batelaan, F. De Smedt, SEEPAGE, a new MODFLOW DRAIN package, Ground Water 42 (2004) 576–588.
[39] A. Chakib, A. Nachaoui, Nonlinear programming approach for transient free boundary flow problem, Appl. Math. Comput. 160 (2005) 317–328.
[40] B. Ataie-Ashtiani, R.E. Volker, D.A. Lockington, Tidal effects on groundwater dynamics in unconfined aquifers, Hydrol. Process. 15 (2001) 655–669.
[41] F.U. Jun-feng, J.I.N. Sheng, A study on unsteady seepage flow through DAM, J. Hydrodyn. 21 (2009) 499–504.
[42] L. Yuanyi, Y. Dekui, L. Binliang, F.-Y. Teo, A fully coupled depth-integrated model for surface water and groundwater flows, J. Hydrol. 542 (2016) 172–184.
[43] C. Di Nucci, Theoretical derivation of the conservation equations for single phase flow in porous media: a continuum approach, Meccanica 49 (2014) 2829–2838.
[44] W. Zijl, M. Nawalany, Natural Groundwater Flow, Lewis Publishers, Boca Raton, 1993.
[45] J. Bear, A.H.D. Cheng, Comment on: "Methods to derive the differential equation of the free surface boundary" by C. Chen, X. Kuang, J.J. Jiao, Ground Water 48 (2010) 486–489.
[46] C. Baiocchi, V. Comincioli, E. Magenes, G.A. Pozzi, Free boundary problems in the theory of fluid flow through porous media, Ann. Mat. Pura Appl. 97 (1973) 1–82.

[47] G.B. Whitham, Linear and Nonlinear Waves, Wiley, New York, 1974.
[48] J.H. Knight, Steady periodic flow through a rectangular DAM, Water Resour. Res. 12 (1981) 1222–1224.
[49] S. Saks, A. Zygmund, Analytic Functions, Elsevier, Amsterdam–London–New York, 1971, https://eudml.org/doc/219298.
[50] S.D. Fisher, Complex Variables, Dover, New York, 1999.
[51] T.B. Benjamin, M.J. Lighthill, On cnoidal waves and bores, Proc. R. Soc. London A 224 (1954) 448–460.
[52] E.M. de Jager, On the origin of the Korteweg–de Vries equation, arXiv:math.HO/0602661.
[53] E. Marchi, A. Rubatta, Meccanica dei Fluidi – Principi e Applicazioni Idrauliche, UTET, Torino, 1996.
[54] E. Marchi, On the free overfall, J. Hydraul. Res. 31 (1993) 777–790.
[55] C. Di Nucci, A. Russo Spena, M.T. Todisco, On the non-linear unsteady water flow in open channels, Il Nuovo Cimento B 122 (2007) 237–255.
[56] D. Dutykh, F. Dias, Dissipative Boussinesq equations, C. R. Mecanique 335 (2007) 559–583.
[57] COMSOL Multiphysics 5.2a, COMSOL Inc., 2016.
[58] C. Caruso, P. Lonetti, A. Manna, Dynamic crack propagation in fiber reinforced composites, in: Proc. COMSOL Conference 2009 Milan, 2009.
[59] I.A. Charni, A rigorous derivation of Dupuit's formula for unconfined seepage with seepage surface, Dokl. Akad. Nauk S.S.S.R. 79 (1951) 937–940 (in Russian).